International Journal of Psychosocial Rehabilitation, Vol. 24, Issue 02, 2020
ISSN: 1475-7192

FEM BASED 3-D SIMULATION AND HARDWARE DESIGN OF POWER AMPLIFIER FOR SINGLE COIL ACTIVE MAGNETIC BEARING

[1]JONATHAN LALDINGLIANA, [2]PABITRA KUMAR BISWAS.

ABSTRACT--*Active Magnetic bearing (AMB) is a bearing which levitates the rotor in the air without any physical contact between the actuator (an electromagnet) and the object (a rotor). For hovering the rotor of AMB in the air it is important to supply the necessary measure of current through the coil. Therefore, proper selection of power amplifier for an AMB system is an absolute necessity. This paper deals with the 3-dimensional simulation of a single-coil AMB (SAMB) system using FEM based software known as ANSYS Maxwell. Magnetic properties such as- flux pattern, flux density, electromagnetic field, inductance and force are obtained in this research work. Various sorts of Power amplifiers are simulated in PSIM for the proposed SAMB system and the most efficient amplifier is designed in hardware for validating the software result.*

KEYWORDS--*Active Magnetic Bearing (AMB), Single coil AMB(SAMB), flux pattern, ANSYS, PSIM, Power amplifier.*

I. INTRODUCTION

Magnetic Bearing (MB) is noncontact bearing, which utilized magnetic force to support the rotor object in the absence of mechanical contact [1]. A magnetic bearing is broughtly divided into two parts- Passive Magnetic Bearing (PMB) that used permanent magnet force or reluctance force to suspends the rotor of a bearing, the force generates by PMB is a fixed force [2],[3]. While the other one is Active Magnetic bearing (AMB) which utilized controlled electromagnetic force. PMB is difficult to design due to the limitation described by Earnshaw's theorem [4]. Methods using diamagnetic materials are relatively undeveloped and strongly depend on material characteristics. Subsequently, most magnetic bearings are active magnetic bearings, using electromagnets force to support the load or the rotor, the force generates by an AMB system can be transformed as desired [2],[5]. Accordingly, in this research study AMB system is selected.

There are numerous pros of an AMB system when contrasted with conventional types of bearing. AMB has contactless motion control characteristic, frictionless, extra high-speed rotation and long life. Because of these attributes, it becomes a key machine in high speed rotating machines industries, gas turbine, compressors, motor, generator and energy storage [6]. The fundamental piecesof an AMB system are- sensor, controller, power amplifier, rotor and actuator [7]. Basicclosed loop diagram of an AMB system is delineated in figure 1.

[1] *National Institute of Technology, Mizoram. Aizawl, Mizoram, India, jonathan.eee.phd@nitmz.ac.in*

[2] *National Institute of Technology, Mizoram. Aizawl, Mizoram, India, , pabitra.eee@nitmz.ac.in*

Received: 02 Dec 2019 | Revised: 24 Jan 2020 | Accepted: 16 Feb 2020

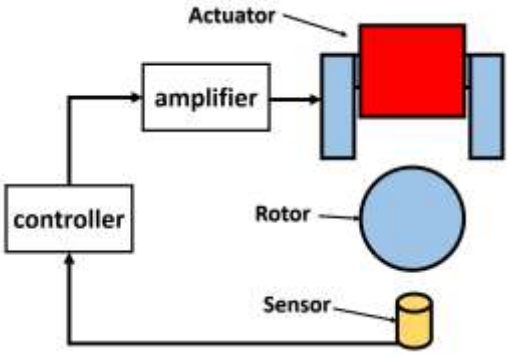

Fig. 1: Block diagram of Active Magnetic Bearing (AMB)

The sensor evaluated the distance between the rotor and the actuator and the detecting signal is sent back to the controller. Rely upon the information acquired by the sensor [8], the controller produces the necessary amount of controlling date for pulsing the gate of the power amplifier. Thusly, the signal from the controller is then intensified by the power-amplifier to create the required amount of force by the actuator of an AMB plant.

II. MATHEMATICAL EXPRESSION OF AN ACTIVE MAGNETIC BEARING.

In a single coil AMB (SAMB) system, when the gravitational pulling force is actually equivalent to the measure electromagnetic force produced by the actuator, the rotor is levitated as illustrated in figure 2. The mathematical expressing has appearedin equation 1 which is non-linear in nature [9].

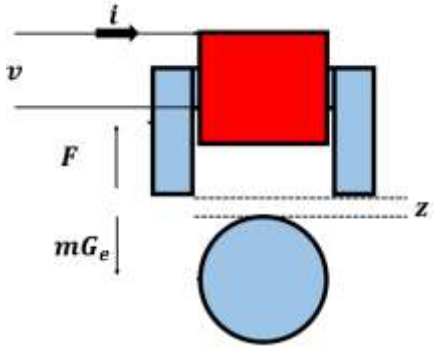

Fig.2: Simplified diagram of AMB

$$m\ddot{z} = mG_e - L\left(\frac{i}{z}\right)^2 \qquad 1$$

Where $'m'$ is the weight of the rotor, $'G_e'$ is the gravitational constant, $'L'$ is an electromagnetic constant and $'i'$ is the coil current.

For proper analysis of an AMB system, the non-linear model is to be linearized.

$$\ddot{z} = G_e - F(i,z) \qquad 2$$

$$F(i,z) = \frac{L}{m}\left(\frac{i}{z}\right)^2 \qquad 3$$

Received: 02 Dec 2019 | Revised: 24 Jan 2020 | Accepted: 16 Feb 2020

By assuming $\ddot{z} = 0$, the equilibrium point is calculated.

$$G_s = F(i, z) = z_0 i_0 \quad 4$$

Using a series expansion method, the linearized equation is obtained.

$$\ddot{z} = -\left(\frac{\partial F(i,z)}{\partial i}\Big|_{i_0,z_0} \Delta i + \frac{\partial F(i,z)}{\partial z}\Big|_{i_0,z_0} \Delta z\right) \quad 5$$

Applying Laplace transform in the above equation we obtain the following equation-

$$s^2 \Delta z = -(L_a \Delta i + L_b \Delta z) \quad 6$$

$$\frac{\Delta z}{\Delta i} = \frac{-L_a}{s^2 + L_b} \quad 7$$

Where, $L_a = \frac{2mG_s}{i_0}$ and $L_b = \frac{2mG_s}{z_0}$.

Therefore, from the equation, the transfer function changes rapidly with the change in gap between the rotor and the actuator.

III. MAGNETIC ANALYSIS OF SINGLE COIL AMB.

Using Finite Element Method(FEM) wide scope of issues in engineering can beinvestigatedsuch as- linear, non-linear problems, fluid flow, heat transfer and electromagnetic problem [10].In this work FEM based software ANSYS Maxwell 17.1 is utilized for comprehending the magnetic properties of Single Coil AMB. Three-dimensional FEM simulation has been carried out to visualize the flux pattern, flux density, magnetic force and field. ANSYS Maxwell software is based on Maxwell's equation of electromagnetism [11]. Maxwell's Maxwell equation in differential form can be marked as-

$$\nabla \mathrm{XE} = -\frac{\partial B}{\partial t} \quad 8$$

$$\nabla \mathrm{XH} = \mathrm{J} + \frac{\partial D}{\partial t} \quad 9$$

$\nabla . \mathrm{B} = 0$ and $\nabla . \mathrm{D} = \rho$. For static magnetic field- $\frac{\partial D}{\partial t} = 0$. Therefore,

$$\nabla \mathrm{XH} = \mathrm{J} \quad 10$$

$B = \mu H = H\mu_0\mu_r$ and $D = \varepsilon E = E\varepsilon_0\varepsilon_r$

$$\nabla . \mathrm{J} = -\frac{\partial \sigma}{\partial t} \quad 11$$

Where, 'J' is the current density, 'E' is the electric field intensity, 'H' is the magnetic field intensity, 'B' is magnetic flux density, 'D' is electric charge density, 'ρ' is volume charge density. 'μ', 'ε', and 'σ' are the permeability, permittivity and electrical conductivity.

The parameters of Single Coil AMB is this paper is given in table 1 and figure 3.

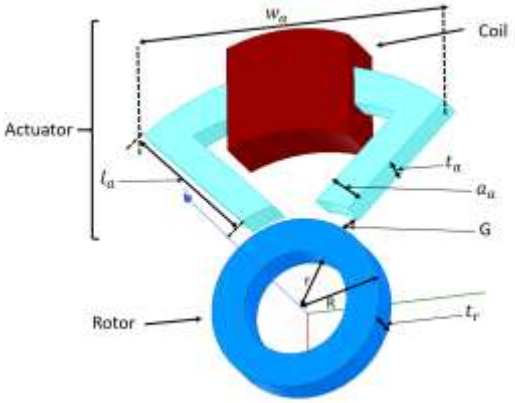

Fig. 3: 3-Dimentional designed of Single Coil AMB using ANSYS Maxwell

Table 1: Parameters of Single coil AMB

Sl. No	Parameter	Unit
1.	Rotor inner radius (r)	25mm
2	Rotor outer radius (R)	40mm
3	Rotor thickness (t_r)	17mm
4	Actuator length (l_a)	90mm
5	Armature width (w_a)	50mm
5	Actuator arm width (a_a)	17mm
6	Actuator arm thickness (t_a)	17mm
7	Number of coil turns (N)	500 turns
8	Weight of rotor (W)	102grams

3-D simulation has been carried out for three different air-gap (10mm, 15mm and 20mm) and the coil current is taken as 3A. Magnetic properties such as flux pattern, magnetic field and electromagnetic force at 10mm air-gap are displayed in figure 4 to figure 6. The 2-D characteristics curves of flux pattern, flux density, magnetic field and force are illustrated in figure 7 to figure 10. It has been discovered that with broadening the airgap between the actuator and the rotorthe linkage flux diminishesdue to the increased in the flux leakage as demonstrated in figure 7.

Received: 02 Dec 2019 | Revised: 24 Jan 2020 | Accepted: 16 Feb 2020

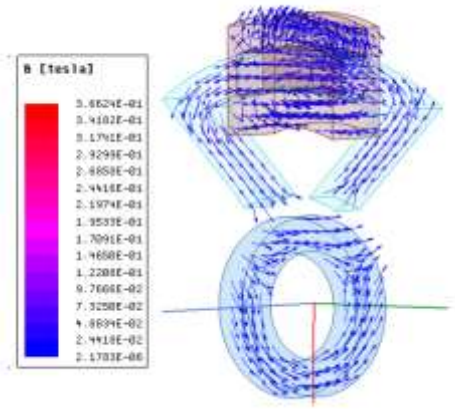

Fig.4: Flux density of single coil AMB at 10mm airgap

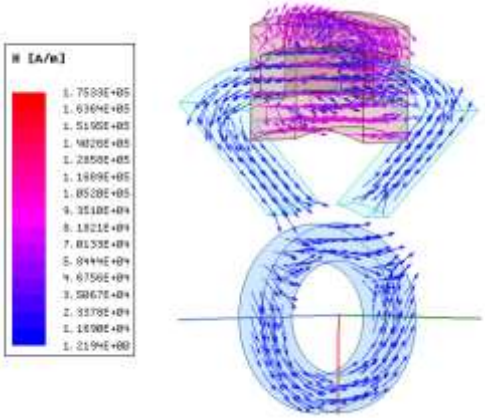

Fig.5Magnetic field intensity of single coil AMB at 10mm airgap

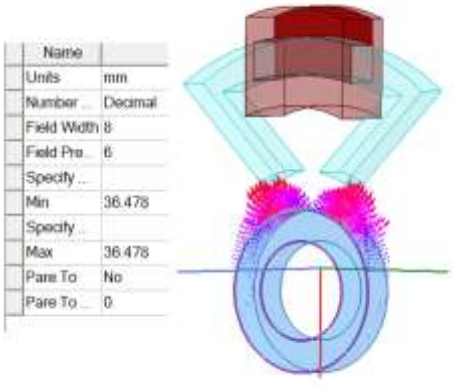

Fig.6: Magnetic field of single coil AMB at 10mm airgap

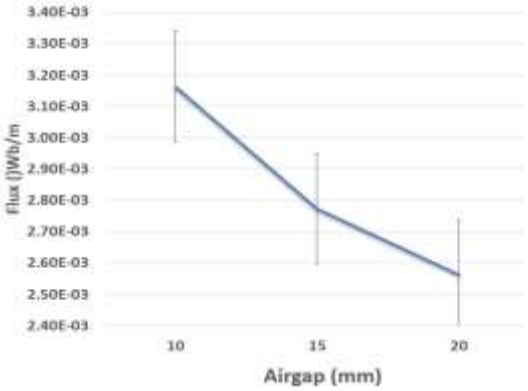

Fig. 7: Characteristics curveof flux with the change in air-gap between actuator and rotor.

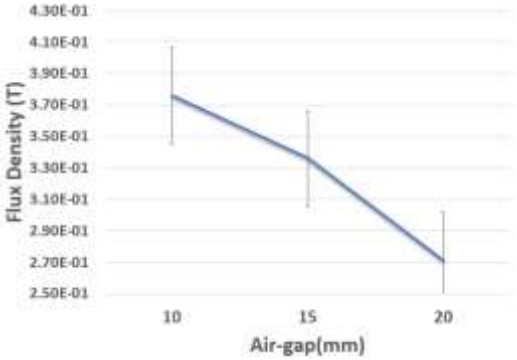

Fig. 8: Characteristics curveof flux density with the change in air-gap between actuator and rotor.

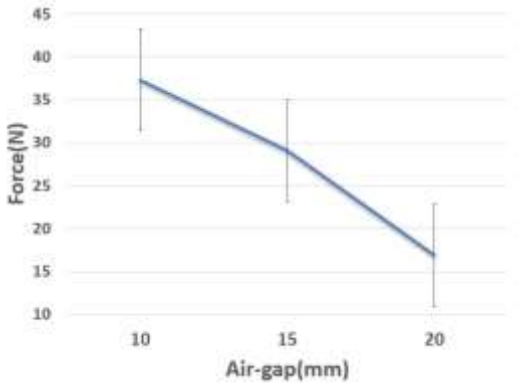

Fig. 9: Characteristics curve of force with the change in air-gap between actuator and rotor.

Received: 02 Dec 2019 | Revised: 24 Jan 2020 | Accepted: 16 Feb 2020

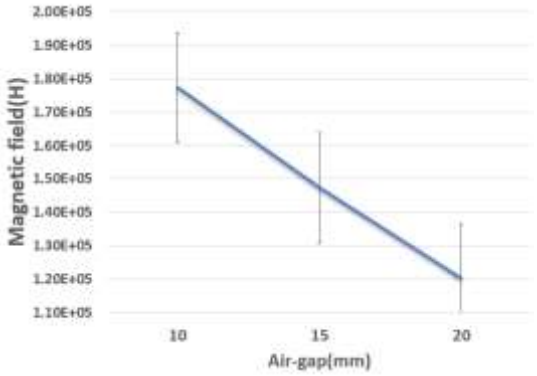

Fig. 10: Characteristics curve of magnetic field with the change in air-gap between actuator and rotor.

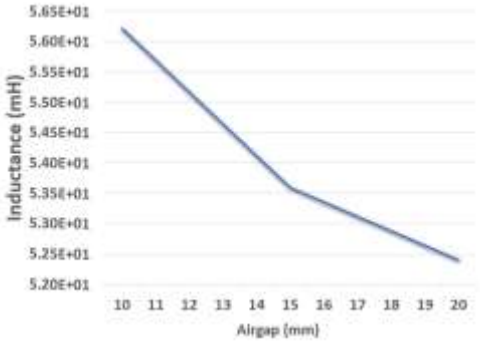

Fig. 11: Inductance vs airgap characteristics.

It has also been observed that with increment in the gap between the rotor and actuator flux density, force and magnetic field continues decreasing. Inductance characteristic curve is illustrated in figure 11, it has been found the value of inductance changed with the adjustment in the gap between the actuator and the rotor. 3-Dimensional plots are illustrated in figure 12 to 14. The 3-D plot between flux and force for three different air-gap is demonstrated in figure 12. Figure 13 shows the graph between force and inductance at the various gap between the actuator and the rotor. While figure 14 shown the graph sketch between the magnetic field and force at various air-gap.

Received: 02 Dec 2019 | Revised: 24 Jan 2020 | Accepted: 16 Feb 2020

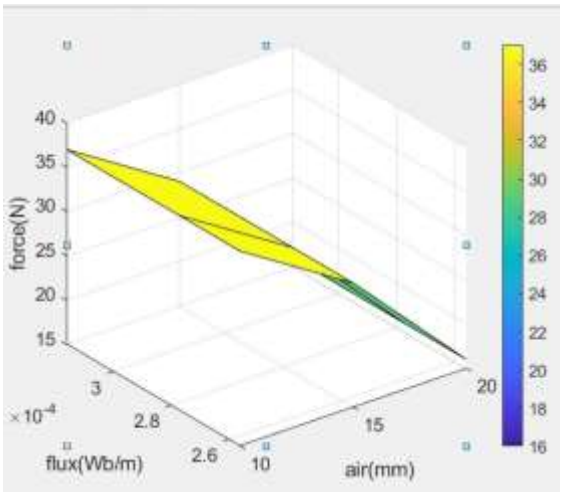

Fig.12: 3-D plot of flux, force and airgap

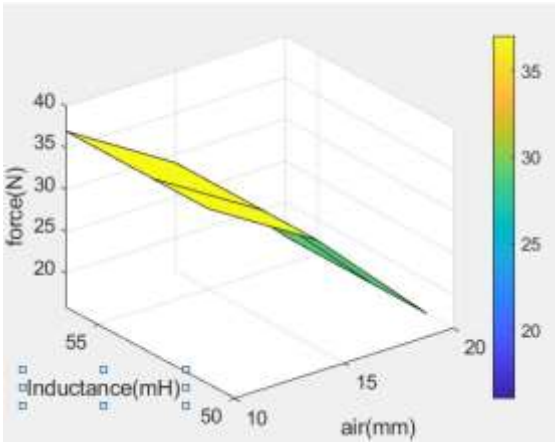

Fig.13: 3-D plot of force, inductance and airgap

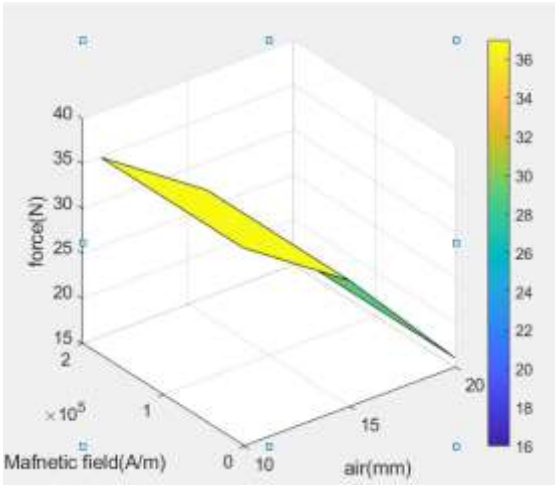

Fig.14: 3-D plot of force, Magnetic field and airgap

IV. SIMULATION OF POWER AMPLIFIER

The transfer function of a real-time model is measured from the hardware setup as appeared in figure 15. Thus, the coil resistance R= 1.4Ω, inductance at 10mm airgap $L_n = 0.0268$H and incremental inductance

$L_o = 0.0087$H. Therefore, the AMB system is expressed as anRL load and the transfer function at 10mm air-gap appears in equation 12.

$$AMB(tf) = \frac{11.9014}{s^2 - 37^2} \quad 12$$

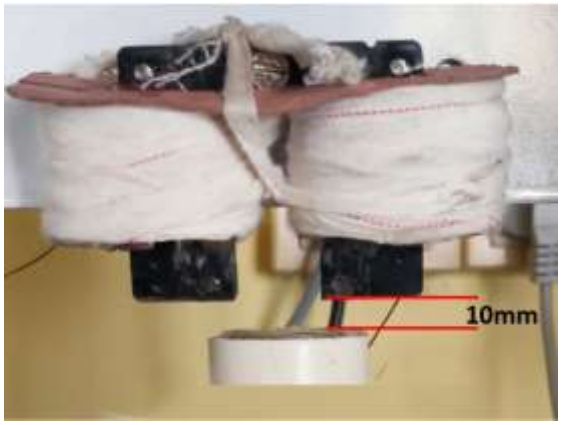

Fig. 15: Real time model of single coil AMB

Since AMB system required bi-polar voltage it is necessary to design a power amplifier which can conveybi-polar voltage. Three sorts of power amplifiers such as buck type, full-bridge type and asymmetrical bridge type power amplifiers are designed for the proposed AMB system using PSIM softwarealongsidethe gate pulsing signals. Buck type power amplifier (figure 16) has one switch when the switch is in OFF condition no voltage is applied to the load while voltage is supply across the load when the switch is in ON condition. The output voltage of a buck type power amplifier is given beneath.

$$V_{out} = D * V_{in} \quad 13$$

Here, 'V_{out}' is the output voltage, 'D' is the duty cycle of the gate pulsing signal and 'V_{in}' is the input voltage to the amplifier.

Full bridge type power amplifier has four switches as shown in figure 17 [12].switches S1 and S2 are triggered at the same time whereas S3 and S4 are worked at another indistinguishable time. When S1 and S2 are triggered, the output current flows across the load through S1 and S2. When S3 and S4 are in ON condition, a current is flowing across the load through S3 and S4.

Asymmetrical bridge type power amplifier is illustrated in figure 18. For this situation,S1 and S2 are operated at the identical time. When S1 and S2 are in ON condition, current flows through the load utilizing the bridge S1 and S2, when both the switches are in off condition current flow through the load utilizing diodes D1 and D2.

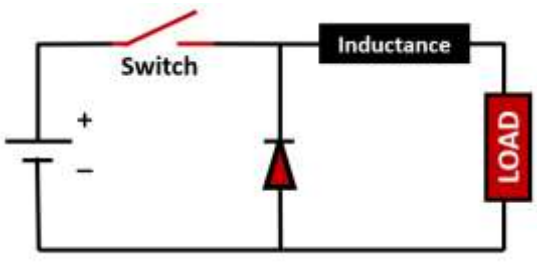

Fig.16: Buck type power amplifier

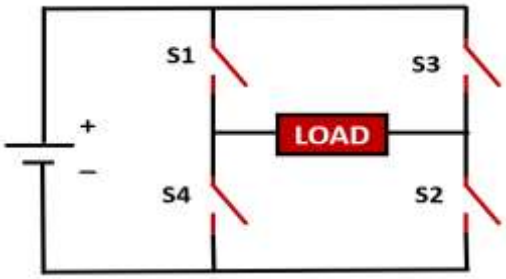

Fig.17: Full bridge type power amplifier.

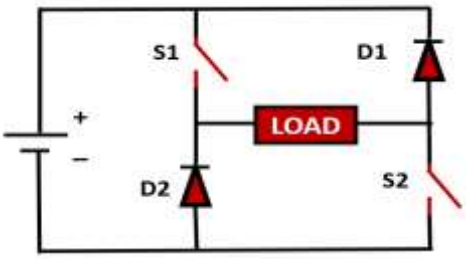

Fig. 18: Asymmetrical bridge type power amplifier.

Simulation has been performed for the selected power amplifiers. Buck type power amplifier along with the Pulse width modulation circuit appears in figure 19. MOSFET switch is utilized in this design, the waveforms such as PWM signal, output voltage and current are given in figure 20. From the output waveform, unipolar voltage is observed which is not fulfilled the requirement of an AMB system. Therefore, a buck type of power amplifier cannot be proceeded further for fabricating in hardware.

Simulation diagram of asymmetrical bridge power amplifier along with the pulse circuit is pictorial in figure 21. In this type of power amplifier, a positive and a negative voltage is seen which is appropriate for an AMB framework (Figure 22). A software model of a full-bridge power amplifier is provided in figure 23. From the simulation results, the bipolar voltage waveform is noticed.

From the simulation results, it has been observed that asymmetrical bridge type and full-bridge type power amplifier are fit for an AMB system. For implement in real-time hardware model asymmetrical bridge type is picked overfull-bridge power amplifier because in full-bridge power amplifier four power switch is desired as well as two units of a pulse generating circuit is required. On the other hand, asymmetrical bridge type power required only two power switches and single pulse generating circuit which is more economical fewer power losses.

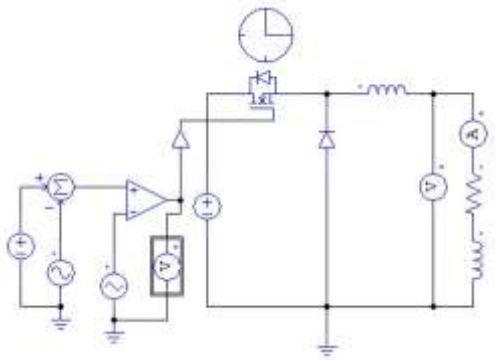

Fig. 19: PSIM circuit of Buck type power amplifier with pulse circuit.

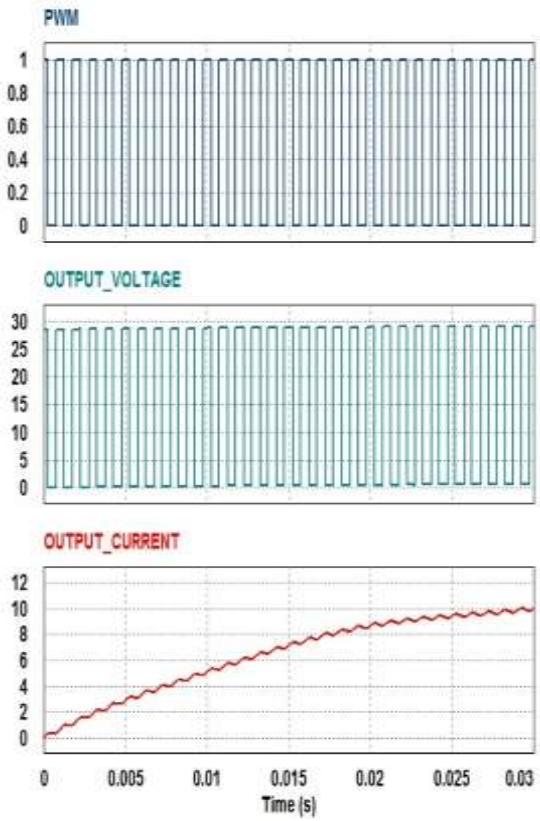

Fig. 20: Pulse signal, output voltage and output current of Buck type Power Amplifier.

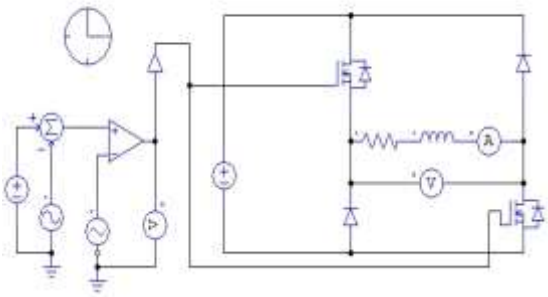

Fig. 21: PSIM circuit of Asymmetrical bridge type

power amplifier with pulse circuit.

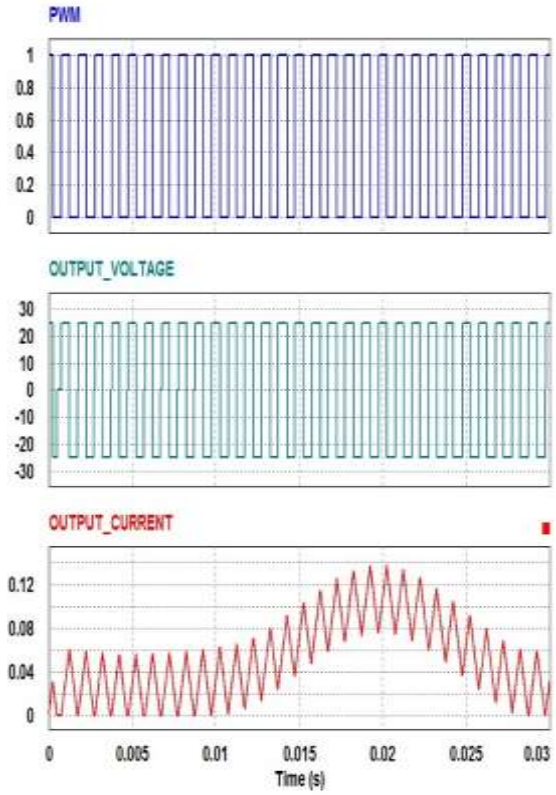

Fig. 22: Pulse signal, output voltage and output current of asymmetrical bridge type Power Amplifier.

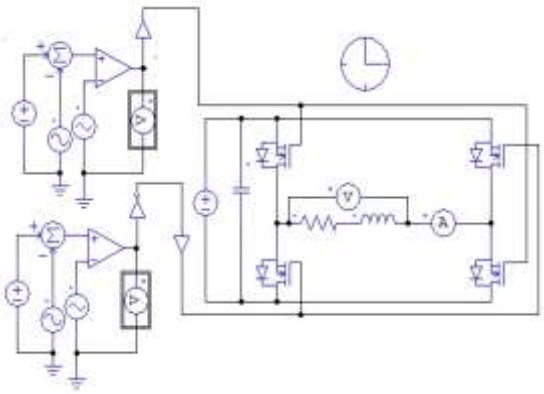

Fig. 23: PSIM circuit full bridge type power amplifier with pulse circuit.

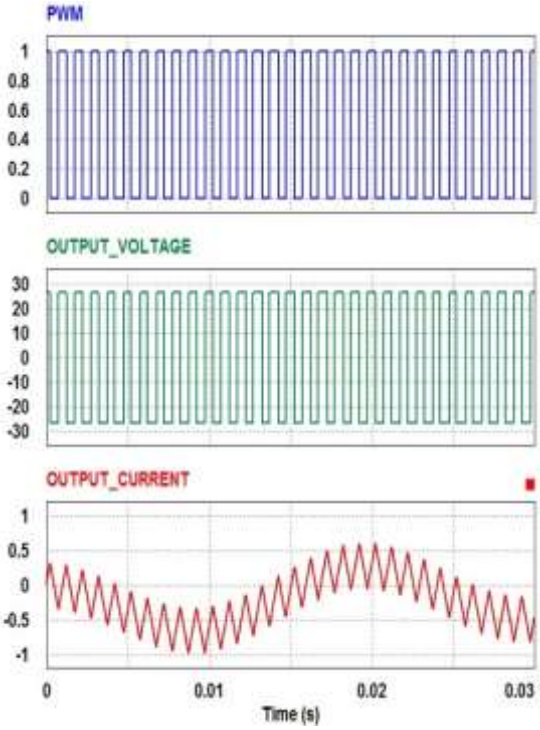

Fig. 24: Pulse signal, output voltage and output current of full bridge type Power Amplifier.

V. HARDWARE DESIGN OF POWER AMPLIFIER

Asymmetrical bridge type power amplifier is fabricated for the proposed single-coil AMB system. In this model, MOSFET IRFP150N is utilized as a power switch and the diode model utilized in this paper is MUR-460 as provided in figure 25. Triangular wave generator has two variable resistors, R1 is used to change the magnitude of the signal whereas the R2 resistor is utilized to change the frequency of the signal. Contingent upon the magnitude provides in the triangular waveform the duty cycle of the gate signal increment or decline.

For hovering an object (rotor) in the air, the high switching frequency is mandatory. Therefore, in this research, the switching frequency is set at 1.97kHz. The ON time period of the gate signal is varied and the corresponding amplifier yield voltage is observed as appeared in figure 25, 26 and 27.

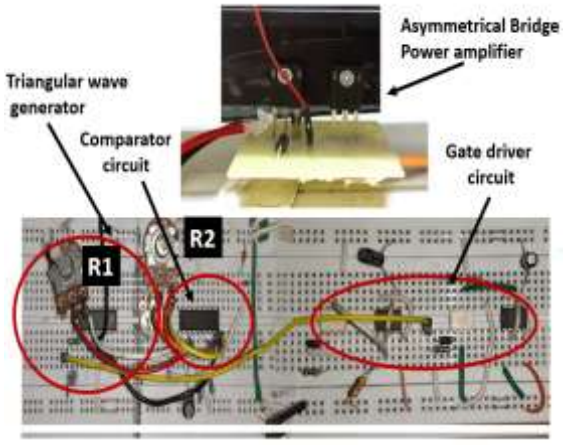

Fig.25: Hardware design of Asymmetrical Bridge type power amplifier.

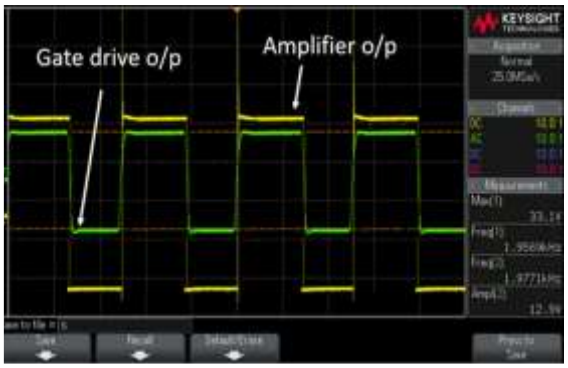

Fig.26: Output waveform of asymmetrical bridge power amplifier (Duty cycle=50%).

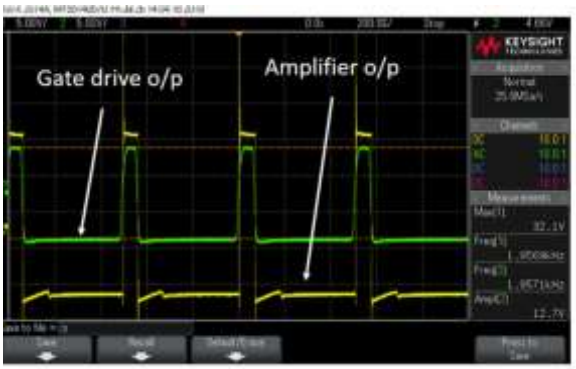

Fig.27: Output waveform of asymmetrical bridge power amplifier (Duty cycle=25%).

VI. CONCLUSION

This work deals with the 3-D modelling and analysis of a proposed Single Coil Active Magnetic Bearing (SAMB) system with ANSYS Maxwell software. Magnetic properties such as flux, flux density, magnetic field and force are obtained for three different air-gaps. From the 2-D characteristic's graphs and 3-D graphs, it has been found magnetic properties continue diminishing when the gap between the rotor and actuator expanded.

In this paper, three shorts of power amplifiers have been designed utilizing PSIM simulation software. From the simulation results, Asymmetrical Bridge type Power Amplifier is favoured over different amplifiers because it accomplishes the requirement of a proposed system as well as cost-effective.

Hardware model of Asymmetrical Bridge type power amplifier along with the pulse circuit has been designed and the corresponding output voltage has been obtained which validated the software results.

REFERENCES

1. Smirnov, Alexander, Nikita Uzhegov, Teemu Sillanpää, Juha Pyrhönen, and Olli Pyrhönen. "High-speed electrical machine with active magnetic bearing system optimization." In IEEE Transactions on Industrial Electronics64, no. 12,pp.9876-9885,2017.
2. Carl R Knospe. "Active magnetic bearings for machining applications." In Control Engineering Practice 15, no. 3, pp.307-313, 2007.
3. Roberto Bassani. "Levitation of passive magnetic bearings and systems." In Tribology International 39, no. 9, pp 963-970, 2006.
4. W Jones. "Earnshaw's theorem and the stability of matter." In European Journal of Physics 1, no. 2, pp.85, 1980.
5. Thomas Schuhmann, Wilfried Hofmann, and Ralf Werner. "Improving operational performance of active magnetic bearings using Kalman filter and state feedback control." In IEEE Transactions on Industrial Electronics 59, no. 2, pp. 821-829, 2011.
6. Ha-Yong Kim, and Chong-Won Lee. "Design and control of active magnetic bearing system with Lorentz force-type axial actuator." In Mechatronics 16, no. 1, pp. 13-20, 2006.
7. Jonathan Laldingliana, Pabitra Kumar Biswas, and Sukanta Debnath. "Magnetic Analysis of Single-Axis Active Magnetic Bearing using ANSYS base Environment." In International Journal of Engineering Technology Science and Research,IJETSR, pp.169-174, 2017.
8. Tom Chang and John Canfield. "Integrated ambient light sensor and distance sensor." InU.S. Patent 8,705,015, issued April 22, 2014.
9. M. Autila, Erkki Lantto, and Antero Arkkio. "Determination of forces and linearized parameters of radial active magnetic bearings by finite element technique." In IEEE Transactions on Magnetics 34, no. 3, pp. 684-694, 1998.
10. A. R. Mitchell, "OF THE FINITE ELEMENT METHOD." In The Mathematics of Finite Elements and Applications: Proceedings of the Brunel University Conference of the Institute of Mathematics and Its ApplicationsHeld in April 1972, Academic Press , pp. 37, 2014.
11. Bo Thidé, "Electromagnetic field theory."In Upsilon Books, 2017.
12. Lingxiao Xue and Ju Zhang. "Full bridge power amplifier with coupled ZVS tanks for wireless power transfer." In U.S. Patent 10,186,971, issued January 22, 2019.

Received: 02 Dec 2019 | Revised: 24 Jan 2020 | Accepted: 16 Feb 2020